

## EXTENDED HI ROTATION CURVE AND MASS DISTRIBUTION OF M31

CLAUDE CARIGNAN<sup>1</sup>, LAURENT CHEMIN<sup>1,2</sup>, WALTER K. HUCHTMEIER<sup>3,4</sup>, AND FELIX J. LOCKMAN<sup>5</sup>  
*Accepted in ApJ Letters*

### ABSTRACT

New HI observations of Messier 31 (M31) obtained with the Effelsberg and Green Bank 100-m telescopes make it possible to measure the rotation curve of that galaxy out to  $\sim 35$  kpc. Between 20 and 35 kpc, the rotation curve is nearly flat at a velocity of  $\sim 226$  km s<sup>-1</sup>. A model of the mass distribution shows that at the last observed velocity point, the minimum dark-to-luminous mass ratio is  $\sim 0.5$  for a total mass of  $3.4 \times 10^{11} M_{\odot}$  at  $R < 35$  kpc. This can be compared to the estimated MW mass of  $4.9 \times 10^{11} M_{\odot}$  for  $R < 50$  kpc.

*Subject headings:* galaxies: halos — galaxies: fundamental parameter (mass) — galaxies: individual (M31) — galaxies: kinematics and dynamics galaxies: structure — Local Group

### 1. INTRODUCTION

Over the last 35 years, accurate rotation curves (RC) have been derived for a large number of galaxies in the Local Universe, using HI or CO at radio wavelengths, or emission lines such as H $\alpha$  in the optical (see Sofue & Rubin 2001, and references therein). With larger telescopes and new instrumentation, RCs have even been measured for galaxies at redshifts  $z \gtrsim 0.5$  (Vogt et al. 1997; Ziegler et al. 2003; Flores et al. 2004; Bamford et al. 2005).

Surprisingly, the two nearest massive galaxies, the Milky Way (MW) and M31 (at an adopted distance of 780 kpc from McConnachie et al. 2005), have very poorly defined RCs. Our position inside the Milky Way's disk makes it very difficult to interpret the HI outside the solar radius, while for M31, the gas on the receding side is at the same velocity as MW gas and it is difficult to disentangle the two components. As importantly, the very large angular size of this galaxy makes it a difficult target for synthesis telescopes (like the VLA) which are not sensitive to emission from large angular scales.

In spite of numerous attempts to determine the dynamical mass of M31, a galaxy rich in globular clusters, satellites, HII regions, planetary nebulae and having an extended HI disk (Hartwick & Sargent 1974; Gunn 1975; Rood 1979; van den Berg 1981; Hodge 1992; Courteau & van den Berg 1999; Merrett et al. 2003; Ibata et al. 2004), mass estimates are quite far from satisfactory. Indeed, we are still uncertain as to whether M31 or the MW is the most massive member of the Local Group (Evans et al. 2000). The kinematics of M31 was studied extensively about 20 - 30 years ago in HI (Roberts & Whitehurst 1975; Emerson 1976; Cram, Roberts & Whitehurst 1980; Unwin 1983; Brinks & Shane 1984) and H $\alpha$  (Rubin & Ford 1970; Boulesteix et al. 1987; Kent 1989). More recent HI synthesis work was done by

Braun (1990) and collaborators using the VLA, WSRT and the GBT (Thilker et al. 2004).

Modern 21 cm HI receivers are up to an order-of-magnitude more sensitive than those used in the earlier surveys, and with 100-m telescopes such as those at Effelsberg and Green Bank, it is now possible to trace the HI in M31 to a significantly larger radius than before. We have thus begun a program of observing 21 cm emission from the outer parts of this galaxy at  $R \geq 90'$  along its major axis. To avoid confusion with Galactic HI, only the approaching (SW) side of the galaxy was observed. The major-axis of M31 has a position angle of  $38^\circ$  and its central position given in the Nasa/Ipac Extragalactic Database is  $\alpha_{J2000} = 00^h42^m44.^s3$ ,  $\delta_{J2000} = +41^\circ16'09''$ . Throughout the article, line-of-sight velocities are given in the heliocentric rest frame.

### 2. OBSERVATIONS

The first observations were obtained with the Effelsberg 100-m telescope which has a HPBW =  $9'.3$ . Spectra were measured every  $4'.5$  along the major axis of the SW (approaching) side, beginning at  $R = 90'$ , or about 20 kpc from the galaxy's center. Spectra were measured modulating between the signal band and a comparison band offset 1.56 MHz, or about  $-300$  km s<sup>-1</sup>. The two-channel HEMT receiver was followed by a 1024 channel autocorrelator split into two bands of 512 channels, with a channel spacing of 0.64 km/s. The system temperature was  $< 30$  K. Both polarizations were averaged to reduce the noise.

The brightest HI emission in M31 comes from a broad, ring-like structure in the inner parts of the galaxy (Emerson 1976; Unwin 1983; Braun 1990), and it is possible that some of this emission might be picked up in a telescope sidelobe (Reich et al. 1978) and mask any weak HI signal from the outer parts of the galaxy. Care was thus taken during the Effelsberg observations to ensure that the main sidelobes in the elevation direction were not falling on the galaxy. Most of the observations were done at parallactic angles  $\sim -45^\circ$  to  $-55^\circ$ , which is  $\sim 90^\circ$  from the M31 major axis.

Sidelobes are less of a problem with the 100-m Green Bank Telescope (GBT), whose offset optics give it a very clean main beam with a first sidelobe level more than 25 dB below the peak. The GBT's gregorian 21 cm receiver system overilluminates the subreflector somewhat, producing a broad forward spillover lobe which contains about 4% of the telescope's total response. However, this sidelobe has a diameter  $> 30^\circ$  on the sky and its effects on the current observations

<sup>1</sup> Laboratoire d'Astrophysique Expérimentale (LAE), Observatoire du mont Mégantic, and Département de physique, Université de Montréal, C.P. 6128, Succ. Centre-Ville, Montréal, Qc, Canada H3C 3J7  
Electronic address: Claude.Carignan@Umontreal.ca

<sup>2</sup> Observatoire de Paris, section Meudon, GEPI, CRNS-UMR 8111 & Université Paris 7, 5 Pl. Janssen, 92195, Meudon, France

<sup>3</sup> Max-Planck-Institut für Radioastronomie, Auf dem Hügel 69, Bonn 53121, Germany

<sup>4</sup> Some of the observations reported here were obtained with the 100 m telescope of the Max-Planck-Institut für Radioastronomie at Effelsberg

<sup>5</sup> National Radio Astronomy Observatory, P.O. Box 2, Green Bank, WV 24944, USA. The National Radio Astronomy Observatory is operated by Associated Universities, Inc., under a cooperative agreement with the National Science Foundation.

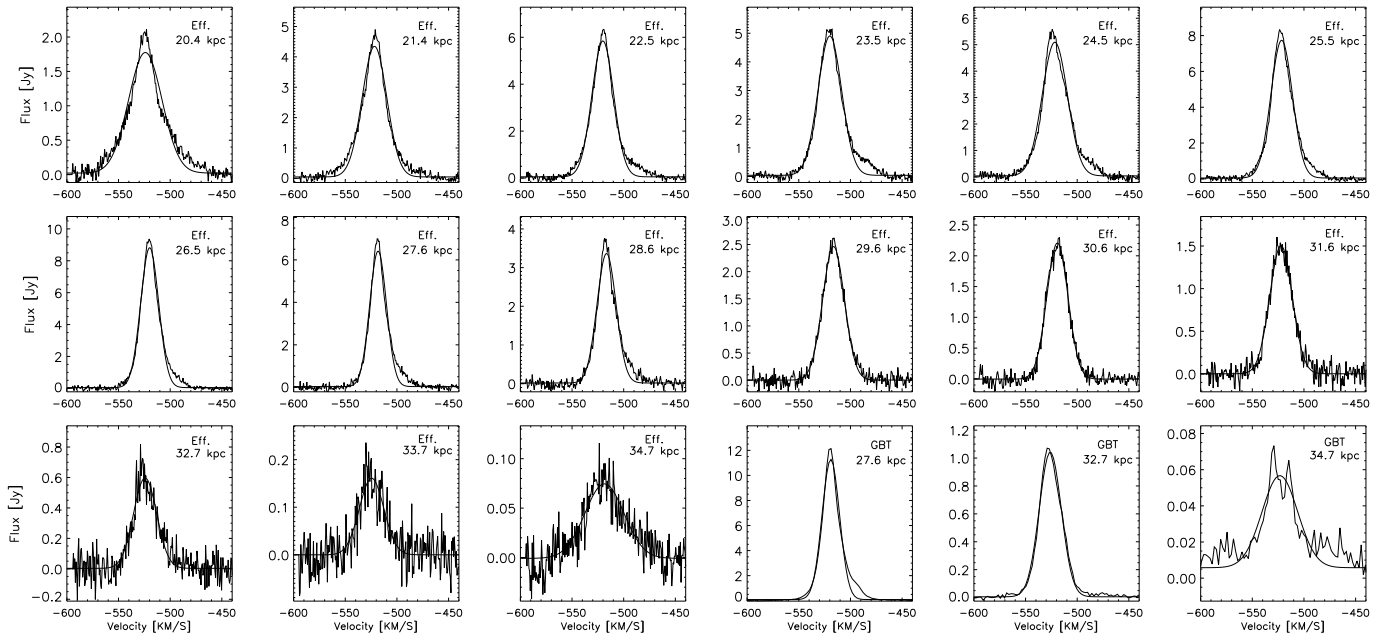


FIG. 1.— HI spectra – baseline subtracted – from the Effelsberg and GBT 100-m radiotelescopes, with their gaussian fits. The radius is given in the top-right corner. These are only the central portions of the observed spectra; we believe that all the emission shown here, including the line wings, is real (cf. the Effelsberg and GBT profiles at 27.6 kpc).

should be negligible (Lockman & Condon 2005).

The GBT was used to measure HI spectra at ten positions along the SW major axis of M31 in August and September 2005. At 21 cm, the GBT has an FWHM angular resolution of  $9''.1$ . Spectra were taken with  $2.5 \text{ km s}^{-1}$  effective velocity resolution over a range  $> 1000 \text{ km s}^{-1}$  centered on the M31 velocity. Frequency switching ‘in band’ gave good instrumental baselines and good sensitivity. The dual-polarization receiver had a system temperature  $T_{\text{sys}} \sim 18 \text{ K}$ . The ten positions were observed for times varying from a few minutes to more than one hour, with a typical value being 40 minutes.

HI emission was detected out to  $R = 45 \text{ kpc}$  with the Effelsberg dish, but here we will discuss only data at  $\leq 35 \text{ kpc}$  where spectra were measured with both Effelsberg and the GBT. Moreover, the HI disk of M31 is known to be slightly warped (e.g. Newton & Emerson 1977; Henderson 1979). Knowing our beamsize and estimates of the warp parameters, we have calculated that HI profiles obtained along a constant line of  $38^\circ$  are reliable only up to 35 kpc.

Within this range the agreement between data from the two telescopes is good. For the positions observed with both telescopes (27.6, 32.7, 34.7 kpc), the mean difference in radial velocity is less than  $2.5 \text{ km s}^{-1}$ , and at these three locations the radial velocity is thus given by the average of the two observations. The HI spectra, baseline subtracted, with the best fit Gaussian profile superposed, are shown in Figure 1. While there is some scaling differences between the profiles coming from the two telescopes, the profile shapes are remarkably similar (e.g., the two spectra at  $R = 27.6 \text{ kpc}$ ).

### 3. ROTATION CURVE OF M31

There are discrepancies between the different determinations of the RC of M31 in the inner 10 kpc (Sofue & Kato 1981), but there is general agreement for  $10 \leq R \leq 30 \text{ kpc}$ . One interesting feature of the HI RC of M31 is that it seems to be declining more or less regularly from the center all the way out to 30 kpc (Braun 1991). While there are a few galaxies with declining RCs over a limited radius range (Carignan

TABLE 1  
HI ROTATION VELOCITIES COMPUTED FROM DATA IN UNWIN (1983) FOR THE INNER PARTS ( $R \leq 90'$ ) AND FROM THE EFFELSBERG AND GBT SINGLE DISH OBSERVATIONS FOR THE OUTER PARTS ( $R > 90'$ ).

Radius (1)	Radius (2)	$V_{\text{rot}}$ (3)	$\Delta V_{\text{rot}}$ (3)	Radius (1)	Radius (2)	$V_{\text{rot}}$ (3)	$\Delta V_{\text{rot}}$ (3)
25.0	5.68	235.5	17.8	94.5	21.45	227.6	28.8
30.0	6.81	242.9	0.8	99.0	22.47	226.0	28.8
35.0	7.95	251.1	0.7	103.5	23.50	225.7	28.8
40.0	9.08	262.0	2.1	108.0	24.52	227.5	28.8
45.0	10.22	258.9	6.9	112.5	25.54	227.4	28.8
50.0	11.35	255.1	5.7	117.0	26.56	225.6	28.8
55.0	12.49	251.8	17.1	121.5	27.58	224.4	28.8
60.0	13.62	252.1	7.4	126.0	28.60	222.3	28.8
65.0	14.76	251.0	18.6	130.5	29.62	222.1	28.8
70.0	15.89	245.5	28.8	135.0	30.65	224.9	28.8
75.0	17.03	232.8	1.0	139.5	31.67	228.1	28.8
80.0	18.16	232.0	14.2	144.0	32.69	231.1	28.8
85.0	19.30	235.7	4.6	148.5	33.71	230.4	28.8
90.0	20.43	229.3	13.8	153.0	34.73	226.8	28.8

Notes on columns: (1) and (2) Radius in arcmin and kpc (resp.) for  $D = 780 \text{ kpc}$  (McConnachie et al. 2005) ( $1' = 227 \text{ pc}$ ); (3): Velocity in  $\text{km s}^{-1}$ , for a systemic velocity of  $-300 \text{ km s}^{-1}$  (de Vaucouleurs et al. 1991).

& Puche 1990; Casertano & van Gorkom 1991; Honma & Sofue 1997), this is quite unlike what is seen in most spirals, and is one of the reasons we wished to obtain the velocity information at larger radii to check whether that trend continues.

Table 1 and Figure 2 give our derived HI RC. For  $R \leq 90'$  (or  $\sim 20.5 \text{ kpc}$ ), we have redetermined the HI velocity field using the early HI data-cube of Unwin (1983) and recomputed the rotation velocities by fitting a tilted-ring model to the velocity map. The *rotcur* task (Begeman 1989) of the GIPSY package (van der Hulst et al. 1992) was used for that purpose. No velocities are given inside a radius of  $25'$ , where the deficiency of neutral gas introduces large uncertainties, and where it is probable that there are large non-circular motions. The error-bars for the inner RC are given by the difference between the velocities of the approaching and receding

sides of the galaxy, except for the very few points where the formal error given by *rotcur* is chosen because it exceeds this difference.

The inner part of the new RC compares well with the composite one presented in Widrow et al. (2003), which was compiled from several data sets. The curves of the receding and approaching halves are shown to illustrate the symmetry of the gas motions in the galaxy: except, perhaps, near  $R \sim 70'$  where a difference of  $\sim 29 \text{ km s}^{-1}$  is observed, similar values are derived for the two sides of the galaxy. This asymmetry was also observed in previous HI data (Braun 1991).

The points at  $R > 90'$  were computed from the new single-dish spectra, using the same inclination as for the inner parts ( $77^\circ$ ) and a systemic velocity of  $-300 \text{ km s}^{-1}$  (de Vaucouleurs et al. 1991). The associated errors are taken to be equal to the largest error found in the inner part of the curve. The most striking feature of our new curve is that, far from having a declining RC (Braun 1991), the velocities between 20 and 35 kpc are found to remain nearly constant at  $\sim 226 \text{ km s}^{-1}$ .

Models of the M31 warp at large radii imply a slightly increasing inclination and decreasing position angle of the major axis as a function of radius (Newton & Emerson 1977; Briggs 1990). As a consequence, use of a constant inclination of  $77^\circ$  instead of a higher one at large  $R$  could lead to an overestimate of the rotation velocities, but only at most 2.5% (or  $6 \text{ km s}^{-1}$ ) with respect to the purely edge-on case. As for the position angle, if the HI spectra are not taken exactly along the major axis, the derived velocities would be an underestimate of the true rotational velocity. This strengthens our conclusion that the RC is not declining. Finally, the adopted error of  $\pm 29 \text{ km s}^{-1}$  is very conservative, and likely an overestimate of the errors which might arise, e.g., from a bad choice of the orientation parameters.

Braun's conclusion that the M31 RC was declining at  $R > 100'$  was probably determined by his two points at the greatest  $R$ , which were measured very close to the galaxy's minor axis (Tab. 3 and Fig. 8 of Braun 1991). For such an highly inclined galaxy, the outer regions close to the minor axis suffer from large deprojection errors. Furthermore, the superposition of several gas orbits along the line-of-sight due to the external warp is very important close the minor axis. These effects may lead to a bad estimate of the rotational velocity for the last two points of Braun's RC. A constant velocity at large radii, as the trend we derive, is in agreement with the flat RC model proposed by Brinks & Burton (1984).

#### 4. MASS DISTRIBUTION OF M31

In order to model the mass distribution of M31 using the RC shown in Fig. 2, the luminosity profiles of the luminous components (bulge & disk) were derived from the  $B$ -band parameters given in Walterbos & Kennicutt (1987, 1988). The HI radial profile of Sofue & Kato (1981) was used for the gaseous disk, multiplied by a factor of 4/3 to account for Helium. The observed colors ( $0.8 < (B-V) < 1.0$ ), combined with population models, lead to a value for the stellar component of  $2.8 < (M/L_B) < 6.5$  (Bell & de Jong 2001).

Figure 2 shows the best-fit mass model for M31. The model is described in Carignan (1985), and has a dark matter (DM) component represented by an isothermal sphere. A  $(M/L_B)$  of 7.5 (in units of  $M_\odot/L_\odot$ ) is derived for the stellar disk. This is somewhat higher than the value expected from the colors, which means that this can be considered as a lower limit for the DM component (maximum disk model). Such large  $(M/L_B)$  values from best-fit models are not uncommon:

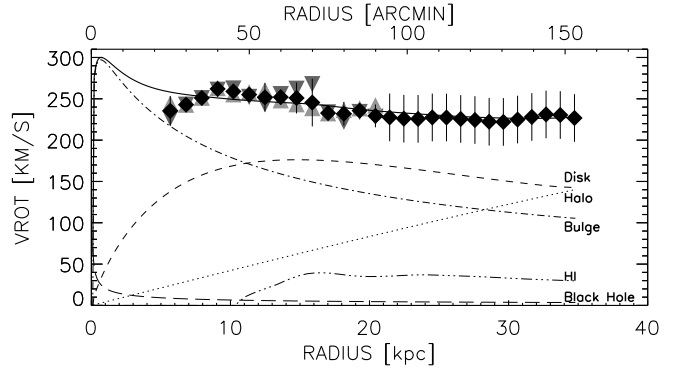


FIG. 2.— Rotation curve and mass model for M31. The new rotation velocities from the Effelsberg and GBT 100-m observations are for  $R > 21$  kpc. The velocities for  $R \leq 21$  kpc are recomputed from the Unwin (1983) HI data. The upper pointing triangles (light grey) are for the receding side and the bottom pointing (dark grey) ones for the approaching side, as obtained from a tilted-ring model (see text). The solid line is the best fit to the data. Each mass component is identified. A mass of  $1.0 \times 10^8 M_\odot$  is used for the central black hole (Bender et al. 2005).

for example, values of 9.4 (Begeman 1989) and 8.5 (Blais-Ouellette et al. 1999) have been found for the galaxy NGC 3198. Comparable estimates of  $(M/L_B)$  have been found from measurements of the vertical stellar velocity dispersion in the nearly face-on galaxies NGC 628 and NGC 1566 (van der Kruit & Freeman 1984).

For  $R < 35$  kpc, the model gives a stellar mass  $\mathcal{M}_{stellar} = 2.3 \times 10^{11} M_\odot$ , an HI mass  $\mathcal{M}_{HI} = 5.0 \times 10^9 M_\odot$ , and a dark matter mass of  $\mathcal{M}_{DM} = 1.1 \times 10^{11} M_\odot$ , leading to a total mass of  $\mathcal{M}_{tot} = 3.4 \times 10^{11} M_\odot$ . This translates in a  $\mathcal{M}_{dark}/\mathcal{M}_{lum} \sim 0.5$  and a total dynamical mass-to-light ratio  $(M/L)_{dyn} \sim 6$  at the last observed velocity point.

#### 5. CONCLUSIONS AND FUTURE WORK

The main conclusions of this Letter are:

- The present study has extended the measured rotation curve of M31 out to  $\sim 35$  kpc. Contrary to previous studies (Braun 1991), the RC does not decline steadily from the center out to the last velocity point but remains nearly constant at  $\sim 226 \text{ km s}^{-1}$  for  $20 \lesssim R \lesssim 35$  kpc.
- A total mass for M31 of  $3.4 \times 10^{11} M_\odot$  is derived for  $R \lesssim 35$  kpc. This is very similar to the mass of  $2.8 \times 10^{11} M_\odot$  (for  $R < 31$  kpc) found using kinematical data of planetary nebulae (Evans & Wilkinson 2000), and can be compared with the MW mass of  $4.9 \pm 1.1 \times 10^{11} M_\odot$  within 50 kpc (Kochanek 1996).
- A study of the mass distribution gives a lower limit to the ratio  $\mathcal{M}_{dark}/\mathcal{M}_{lum} \sim 0.5$  at the last observed velocity point. This is quite different from the no Dark Matter model of Braun (1991).

This study is the first part of a program to derive the best possible rotation curve for M31. Our observations confirm that HI can still be detected past 30 kpc and that the outer RC is flat and not declining. An ideal RC will combine the following two data sets:

(1) *High resolution optical 3-D H $\alpha$  kinematical data.* These data will be obtained with the Fabry-Perot system FANTOMM (Gach et al. 2002; Hernandez et al. 2003). With the  $\sim 14 \times 14$  arcmin<sup>2</sup> field-of-view at the Mont Mégantic Observatory telescope, it will be possible to get a mosaic of the whole optical disk with  $\sim 20$  fields. This will allow us to

get sufficient spatial resolution in the crucial rising part of the RC (Blais–Ouellette et al. 1999) and at the same time provide the 2–D coverage necessary to derive properly the kinematical parameters.

(2) *Arc-minute resolution, high sensitivity synthesis HI data.* Because of the lack of short spacings, the VLA observations (Braun 1990) are not sensitive to the large scale HI structures expected in M31. However, the DRAO synthesis array is sensitive to such structures and retrieves most of the HI present in M31. This has proved to be the case for very extended nearby systems such as NGC 6946 (Carignan et al. 1990) and DDO 154 (Carignan & Beaulieu 1989).

These observations are in progress and should provide the optimal kinematical information for the best possible study of the mass distribution in M31.

We would like to thank O. Hernandez, O. Daigle, M.-H. Nicol, M.-M. de Denus Baillargeon and D. Naudet for useful discussions and an anonymous referee for valuable suggestions. LC acknowledges partial support from the Fonds Québécois de Recherche sur la Nature et les Technologies and CC from the Conseil de Recherches en Sciences Naturelles et en Génie du Canada.

#### REFERENCES

- Bamford, S. P., Milvang-Jensen, B., Aragon-Salamanca, A., & Simard, L., 2005, *MNRAS*, 361, 109
- Begeman, K. G. 1989, *A&A*, 223, 47
- Bell, R. F., & de Jong, R. 2001, *ApJ*, 550, 212
- Bender, R., Kormendy, J., Bower, G., Green, R., Thomas, J., Danks, A. C., Gull, T., Hutchings, J. B., Joseph, C. L., Kaiser, M. E., Lauer, T. R., Nelson, C. H., Richstone, D., Weistrop, D., & Woodgate, B., 2005, *ApJ*, 631, 280
- Blais–Ouellette, S., Carignan, C., Amram, P., & Côté, S. 1999, *AJ*, 118, 2123
- Boulesteix, J., Georgelin, Y. P., Lecoarer, E., Marcelin, M., & Monnet, G. 1987, *A&A*, 178, 91
- Braun, R. 1990, *ApJS*, 72, 755
- Braun, R. 1991, *ApJ*, 372, 54
- Briggs, F. H. 1990, *ApJ*, 352, 15
- Brinks, E., & Burton, W. B. 1984 *A&A*, 141, 195
- Brinks, E., & Shane, W. W. 1984 *A&AS*, 55, 179
- Carignan, C., 1985, *ApJ*, 299, 59
- Carignan, C., & Beaulieu, S. 1989, *ApJ*, 347, 760
- Carignan, C., & Puche, D. 1990, *AJ*, 100, 394
- Carignan, C., Charbonneau, P., Boulanger, F., & Viallefond, F. 1990, *A&A*, 234, 43
- Casertano, S., & van Gorkom, J. H. 1991, *AJ*, 101, 1231
- Courteau, S., & van den Berg, S. 1999, *AJ*, 118, 337
- Cram, T. R., Roberts, M. S., & Whitehurst, R. N. 1980, *A&AS*, 40, 215
- de Vaucouleurs, G., de Vaucouleurs, A., Corwin, H.G., Buta, R.J., Paturel G., & Fouqué, P. 1991, *Third Reference Catalogue of Bright Galaxies* (Springer, New York) (RC3)
- Emerson, D. T. 1976, *MNRAS*, 176, 321
- Evans, N. W., & Wilkinson, M. I. 2000, *MNRAS*, 316, 929
- Evans, N. W., & Wilkinson, M. I., Guhathakurta, P., Grebel, E. K., & Vogt, S. S. 2000, *ApJ*, 540, L9
- Flores, H., Puech, M., Hammer, F., Garrido, O., & Hernandez, O. 2004, *A&A*, 420, L31
- Gach, J.-L., Hernandez, O. Boulesteix, J., Amram, P., Boissin, O., Carignan, C., Garrido, O., Marcelin, M., Östlin, G., Plana, H., & Rampazzo, R. 2002, *PASP*, 114, 1043
- Gunn, J. 1975, *Comments Astrophys. Space*, 6, 7
- Hartwick, F., & Sargent, W. 1974, *ApJ*, 190, 283
- Henderson, A. P. 1979, *A&A*, 75, 311
- Hernandez, O., Gach, J., Carignan, C., & Boulesteix, J. 2003, *Proc. SPIE*, 4841, 1472
- Hodge, P. 1992, *The Andromeda Galaxy*, Kluwer Academic Press, Dordrecht
- Honma, M., & Sofue, Y. 1997, *PASJ*, 49, 539
- Ibata, R., Chapman, S., Ferguson, A. M. N., Irwin, M., Lewis, G., & McConnachie, A., 2004, *MNRAS*, 351, 117
- Kent, S. M. 1989, *PASP*, 101, 489
- Kochanek, C. S. 1996, *ApJ*, 457, 228
- Lockman, F. J., & Condon, J. J. 2005, *AJ*, 129, 1968
- McConnachie, A. W., Irwin, M. J., Ferguson, A. M. N., Ibata, R. A., Lewis, G. F., & Tanvir, N. 2005, *MNRAS*, 356, 979
- Merrett H. R., Kuijken, K., Merrifield, M. R., Romanowsky, A. J., Douglas, N. G., Napolitano, N. R., Arnaboldi, M., Capaccioli, M., Freeman, K. C., Gerhard, O., Evans, N. W., Wilkinson, M. I., Halliday, C., Bridges, T. J., & Carter, D., 2003, *MNRAS*, 346, L62
- Newton, K., & Emerson, D. T. 1977 *MNRAS*, 181, 573
- Reich, W., Kalberla, P., Reif, K., & Neidhöfer, J. 1978, *A&A*, 69, 165
- Roberts, M. S., & Whitehurst, R. N. 1975, *ApJ*, 201, 327
- Rood, H.J. 1979, *ApJ*, 232, 699
- Rubin, V. C., & Ford, W. K. 1970, *ApJ*, 159, 379
- Sofue, Y., & Kato, T. 1981, *PASJ*, 33, 449
- Sofue, Y., & Rubin, V.C. 2001, *ARA&A*, 39, 137
- Thilker, D. A., Braun, R., Walterbos, R. A. M. et al. 2004, *ApJ*, 601, L39
- Unwin, S. C. 1983, *MNRAS*, 205, 787
- van den Berg, S. 1981, *PASP*, 93, 428
- van der Hulst, J. M., Terlouw, J. P., Begeman, K. G., Zwitsers, W., & Roelfsema, P. R., 1992, *ASP Conf. Series*, 25, 131
- van der Kruit, P. C., & Freeman, K. C., 1984, *ApJ*, 278, 81
- Vogt, N. P., Phillips, A. C., Faber, S. M., Gallego, J., Gronwall, C., Guzman, R., Illingworth, G. D., Koo, D. C., & Lowenthal, J. D., 1997, *ApJ*, 479, L121
- Walterbos, R. A. M., & Kennicutt, R. C. 1987, *A&AS*, 69, 311
- Walterbos, R. A. M., & Kennicutt, R. C. 1988, *A&A*, 198, 61
- Widrow, L. M., Perrett, K. M., & Suyu, S. H., 2003, *ApJ*, 588, 311
- Ziegler, B. L., Böhm, A., Jäger, K., Heidt, J., & Möllenhoff, C., 2003, *ApJ*, 598, L87